

Important photochemical processes in the atmosphere*

Geert K. Moortgat

Max-Planck-Institut für Chemie, Atmospheric Chemistry Department, P.O. Box 3060,
D-55020 Mainz, Germany

Abstract: Among the many important roles played by ozone in the atmosphere is the role it plays in the generation of OH radicals, which are responsible for initiating the oxidation of a wide variety of atmospheric trace constituents. The OH production occurs dominantly from the formation of the excited O(¹D) species in the UV photolysis of ozone, followed by the reaction of O(¹D) with H₂O vapor. The photochemistry of ozone is very complex, as the relatively weak bonds in ozone allow different states of the O and O₂ photoproducts to be accessed. Recent detailed studies have now revealed that different photolysis channels are occurring in the 290–375 nm spectral range, the region of importance for the generation of OH radicals in the lower atmosphere. The measured temperature-dependent quantum yields for the production of O(¹D) atoms reflect the importance of the longer “wavelength tail” formation with regard to the enhanced OH production. Other significant atmospheric photolysis processes involving carbonyl compounds are reported. Direct photodissociation rates were measured in the outdoor photoreactor EUPHORE in Valencia and compared with model calculations. For most of the carbonyl compounds the effective quantum yields are significantly below unity.

PHOTOLYSIS OF OZONE: YIELD OF O(¹D)

Among the many important roles played by ozone in the atmosphere is the role it plays in the generation of OH radicals, which are responsible for initiating the oxidation of a wide variety of atmospheric trace constituents (e.g., organic compounds, reduced sulphur species, etc.), thereby removing them from the atmosphere [1]. While photolysis of ozone in the peak of the Hartley (200–300 nm) bands is important for the stratospheric chemistry of ozone, absorption of ozone in the Huggins bands at $\lambda > 300$ nm dominates the photochemical activity in the troposphere and the lower stratosphere. In this region, the OH production occurs dominantly from the formation of the excited O(¹D) species in the UV photolysis of ozone, followed by the rapid reaction of O(¹D) with H₂O vapor: O(¹D) + H₂O → 2OH. Thus, the O(¹D) production rate will depend on the photolysis frequency $J_{(O^{1D})}$ and the ozone concentration. $J_{(O^{1D})}$ is given by the product of the actinic flux F , the ozone absorption cross section, σ , and the O(¹D) quantum yield $\phi_{O^{1D}}$, all of which are wavelength dependent:

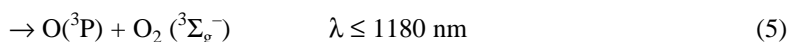
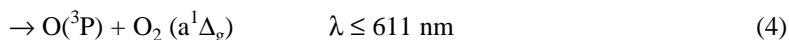
$$J_{O^{1D}} = \int F(\lambda) \cdot \sigma(\lambda) \cdot \phi_{O^{1D}}(\lambda) \cdot d\lambda$$

Above 290 nm, the O(¹D) production rate is a critical component for model calculations: the solar actinic flux increases by more than four orders of magnitude, the temperature-dependent O₃ absorption cross sections in the structured Huggins bands drop from 10⁻¹⁹ to 10⁻²³ cm² molecule⁻¹, and the tem-

*Lecture presented at the XVIIIth IUPAC Symposium on Photochemistry, Dresden, Germany, 22–27 July 2000. Other presentations are published in this issue, pp. 395–548.

perature-dependent O(¹D) quantum yield decreases sharply with increasing wavelengths. Thus, even small changes in the quantum yield in this region affect the O(¹D) production rate.

The photochemistry of ozone is very complex, as the relatively weak bonds in ozone allow different states of the O (³P and ¹D) and O₂ (³Σ_g⁻, ¹Δ_g, and ¹Σ_g⁺) photoproducts to be accessed. Above 290 nm, there are five thermodynamically allowed photolysis channels, shown with their wavelength threshold (at 0 K):



Ozone photolysis dominates throughout the intense Hartley absorption band via the spin-allowed process (1), with a reported O(¹D) quantum yield in the range 0.9 to 0.95. The O(¹D) quantum yield drops to zero below the thermodynamic threshold at 310 nm, since the other (O(¹D)) producing channel (2) is spin-forbidden. However the exact shape of the O(¹D) quantum yield curve at $\lambda > 310$ nm has been the subject of many experimental [2–14] and theoretical [15] studies over the last two decades, leading to controversial results. In particular, the existence of a longer wavelength “O(¹D) quantum yield tail” has now been established over the temperature range 312–227 K [13] and is now recommended for atmospheric calculations [16]. Essentially, the experimentally measured O(¹D) quantum yield tail is consistent with the participation of the temperature-dependent spin-allowed process (1) of vibrationally and rotationally excited ozone in the range 305 to 325 nm, and the temperature-independent constant spin-forbidden process (2) contributing with a constant value of about 0.06. The latter process was found to extend exclusively to 375 nm at 295 K, consistent with absorption to a single excited state [14]. In these measurements [12–14] the production and detection of OH radicals as spectroscopic marker for O(¹D) was used, and revealed to be directly correlated with the ozone absorption cross sections. This recent study suggested that the O(¹D) yield may be constant out to the thermodynamic threshold at 411 nm, however studies were inconclusive due to unreliable O₃ absorption cross sections above 340 nm. [17–19]. The importance of the longer “wavelength tail” in the O(¹D) formation has been confirmed by comparing *in situ* J_(O1D) measurements using spectroradiometric and/or chemical actinometers with calculated photolysis frequencies [1,13,20]. The new recommended temperature-dependent O(¹D) quantum yields (including the tail) yield substantially larger O(¹D) (and consequently larger OH) production rates especially at higher solar zenith angles, low temperatures, and large overhead ozone columns [14], particularly at high latitudes in the troposphere from late autumn to early spring.

PHOTOLYSIS OF CARBONYL COMPOUNDS

Other significant species, producing HO_x (OH, HO₂) species upon photolysis in the atmosphere, include HONO, H₂O₂, CH₃OOH, and carbonyl compounds (mainly aldehydes and ketones). The latter are emitted as primary pollutants (combustion, vegetation) or are produced as reaction intermediates from NO_x-mediated photooxidation of volatile organic compounds (VOCs) emitted into the atmosphere. It is well established that the main degradation processes of carbonyl compounds are controlled by photolysis and/or reaction with OH radicals. The photolysis of these intermediate species is one of the major uncertainties in the VOC oxidation chain in gas-phase atmospheric chemistry.

Because carbonyl compounds produce free radicals as photolysis products, it is important to assess and quantify reliable free radical yields from the photolytic action. This topic was addressed in an EU-funded project "RADICAL" on the photolysis, induced by natural UV/vis solar radiation, of selected carbonyl compounds involved in the atmospheric oxidation of key hydrocarbons. Photodissociation rates of individual carbonyl compounds were measured directly during several campaigns in the EUPHORE outdoor smog chamber (Valencia), and these data were compared with model calculations [21]. The results are summarized in Table 1. Also, the photolytic lifetimes were compared to the lifetime against the OH radical reaction. Effective quantum yields, ϕ_{eff} , were determined by comparison of the individual photolysis frequencies with theoretical decomposition rates using the measured actinic fluxes. For most of the carbonyl compounds the determined ϕ_{eff} is significantly *below unity*.

Table 1 Summary of the photodissociation rates measured at the EUPHORE facility in Valencia.

Compound	Photolytic rate	$J_{\text{calc}} (\phi=1)$	ϕ_{eff}	τ_{phot}	$\tau_{\text{OH}}^{\text{a}}$
Acetaldehyde	$(2.9 \pm 2.7) \times 10^{-6}$	4.9×10^{-5}	0.06 ± 0.05	4 days	17 hours
Propionaldehyde	$(1.1 \pm 0.1) \times 10^{-5}$	3.8×10^{-5}	0.28 ± 0.04	1.2 days	14 hours
Butyraldehyde	$(1.0 \pm 0.2) \times 10^{-5}$	5.1×10^{-5}	0.20 ± 0.04	1.2 days	12 hours
<i>i</i> -Butyraldehyde	$(3.7 \pm 0.1) \times 10^{-5}$	5.2×10^{-5}	0.71 ± 0.02	7.5 hours	11 hours
<i>n</i> -Pentanal	$(1.6 \pm 0.2) \times 10^{-5}$	5.4×10^{-5}	0.30 ± 0.02	17 hours	10 hours
2-Methylbutyraldehyde	$(3.8 \pm 0.1) \times 10^{-5}$	5.2×10^{-5}	0.72 ± 0.03	7.3 hours	12 hours ^b
3-Methylbutyraldehyde	$(1.25 \pm 0.1) \times 10^{-5}$	4.7×10^{-5}	0.27 ± 0.01	22 hours	12 hours ^b
Pivaldehyde	$(1.45 \pm 0.1) \times 10^{-5}$	2.6×10^{-5}	0.56 ± 0.05	19 hours	10 hours
<i>n</i> -Hexanal	$(1.65 \pm 0.3) \times 10^{-5}$	5.9×10^{-5}	0.28 ± 0.05	17 hours	15 hours
<i>n</i> -Nonanal	$(1.15 \pm 0.2) \times 10^{-5}$	4.9×10^{-5}	0.23 ± 0.03	1 day	10 hours
Glyoxal	$(1.05 \pm 0.3) \times 10^{-4}$	2.7×10^{-3}	0.038 ± 0.01	2.6 hours	25 hours
Glycolaldehyde	$(1.14 \pm 0.25) \times 10^{-5}$	8.6×10^{-6}	1.32 ± 0.30	1 day	28 hours
Pyruvic acid	$(1.0 \pm 0.15) \times 10^{-4}$	2.3×10^{-4}	0.43 ± 0.07	2.8 hours	3.2 months
Methylvinylketone	$< \times 10^{-6}$	5.2×10^{-4}	< 0.004	> 6 days	15 hours
Methacrolein	$< \times 10^{-6}$	5.2×10^{-4}	< 0.004	> 6 days	8 hours
Acrolein	$< \times 10^{-6}$	4.3×10^{-4}	< 0.004	> 6 days	13 hours
<i>trans</i> -Crotonaldehyde	$(1.2 \pm 0.15) \times 10^{-5}$	4.0×10^{-4}	0.03 ± 0.01	1 day	7.4 hours
Pinonaldehyde	$(1.15 \pm 0.10) \times 10^{-5}$	8.0×10^{-5}	0.14 ± 0.01	1 day	3.1 hours
Nopinone	3.1×10^{-5}			> 4 days	16 hours
Limonaketone	3.1×10^{-5}			> 4 days	2.0 hours

a) assuming $[\text{OH}] = 1 \times 10^6$ molecule cm^{-3} .

b) OH rate constant from refs. 21 and 22.

The effective quantum yield for C_3 to C_9 straight-chain aldehydes is 0.25 to 0.30, and about twice as large for α -branched aldehydes. The dicarbonyl glyoxal has a very low ϕ_{eff} (0.038), such as found for methylglyoxal in a separate study [23]. For unsaturated compounds (methylvinylketone, methacrolein acrolein, and *trans*-crotonaldehyde) ϕ_{eff} is negligible, although those compounds possess absorption spectra reaching the near visible. The photolytic decay from a few carbonyl compounds derived from the photooxidation from monoterpenes is variable, so need to be determined individually, since absorption spectra are not available. In currently worldwide used atmospheric models, quantum yields are often assumed to be unity, which is seldom the case, as is shown in this study. This leads to an overestimation of the calculated photodissociation rates and the associated radicals formed in photolysis processes. These new data will reduce the present uncertainties associated with photolysis processes, so that future assessments can be made with more confidence.

REFERENCES

1. D. H. Ehhalt. *Phys. Chem. Chem. Phys.* **1**, 5401–5408 (2000).
2. G. K. Moortgat and P. Warneck. *Z. Naturforsch.* **30a**, 835–844 (1975).
3. J. C. Brock and R. T. Watson. *Chem. Phys.* **46**, 477–484 (1980).
4. M. Trolier and J. R. Wiesenfeld. *Geophys. Res. Lett.* **22**, 7119–7124 (1988).
5. W. Armerding, F. J. Comes, B. Schülke. *J. Chem. Phys.* **76**, 3137–3143 (1995).
6. S. M. Ball and G. Hancock. *Geophys. Res. Lett.* **22**, 1213–1216 (1995).
7. K. Takehashi, M. Kishigami, Y. Matsumi, M. Kawasaki, A. J. Orr-Ewing. *J. Chem. Phys.* **105**, 5290–5293 (1996).
8. K. Takehashi, Y. Matsumi, M. Kawasaki, K. Takehashi. *J. Chem. Phys.* **106**, 6390–6397 (1997).
9. K. Takehashi, N. Taniguchi, Y. Matsumi, M. Kawasaki, M. N. R. Ashfold. *J. Chem. Phys.* **108**, 7161–7172 (1998).
10. S. M. Ball, G. Hancock, S. E. Martin, J. C. Pinot de Moira. *Chem. Phys. Lett.* **264**, 531–538 (1997).
11. E. Silvente, R. C. Richter, M. Zheng, A. J. Hynes. *Chem. Phys. Lett.* **264**, 309–315 (1997).
12. R. K. Talukdar, M. K. Gilles, F. Battin-Leclerc, A. R. Ravishankara, J.-M. Fracheboud, J. Orlando, G. S. Tyndall. *Geophys. Res. Lett.* **24**, 1091–1094 (1997).
13. R. K. Talukdar, C. A. Longfellow, M. K. Gilles, A. R. Ravishankara. *Geophys. Res. Lett.* **25**, 143–146 (1998).
14. D. Bauer, L. D’Ottone, A. J. Hynes. *Phys. Chem. Chem. Phys.* **2**, 1421–1424 (2000).
15. H. A. Michelson, R. J. Salawitch, P. O. Wennberg, J. G. Anderson. *Geophys. Res. Lett.* **21**, 2227–2230 (1994).
16. S. P. Sander, R. R. Friedl, W. B. DeMore, D. M. Golden, M. J. Kurylo, R. F. Hampson, R. E. Huie, G. K. Moortgat, A. R. Ravishankara, C. E. Kolb, M. J. Molina. JPL Publication 00-3, Jet Propulsion Laboratory, California Institute of Technology, Pasadena, CA (2000).
17. J. Malicet, D. Daumont, J. Charbonnier, C. Parisse, A. Chakir, J. Brion. *J. Atm. Chem.* **21**, 263–273 (1995).
18. J. Brion, A. Chakir, J. Charbonnier, D. Daumont, C. Parisse, J. Malicet. *J. Atm. Chem.* **30**, 291–299 (1998).
19. S. Voigt, J. Orphal, J. P. Burrows. *Phys. Chem. Chem. Phys.* Submitted for publication.
20. M. Müller, A. Kraus, A. Hofzumahaus. *Geophys. Res. Lett.* **22**, 679–682 (1995).
21. G. K. Moortgat. Final Report of EU-Project ENV4-CT-0419, RADICAL, February 2000.
22. R. Atkinson. *J. Phys. Chem. Ref. Data*, Monograph 2, (1994).
23. S. Koch and G. K. Moortgat. *J. Phys. Chem.* **102**, 9142–9153 (1998).